Clinical Neurophysiology 130 (2019) 1988–1994

Contents lists available at ScienceDirect

Clinical Neurophysiology

journal homepage: www.elsevier.com/locate/clinph

Improvement of motor conduction velocity in hereditary neuropathy of LAMA2-CMD dy^{2J}/dy^{2J} mouse model by glatiramer acetate

Malcolm Rabie [a,b,1], Nurit Yanay [b,1], Yakov Fellig [c], Jenya Konikov-Rozenman [b], Yoram Nevo [a,b,*]

[a] Institute of Neurology, Schneider Children's Medical Center of Israel, Tel-Aviv University, 14 Kaplan Street, Petach Tikva 49202, Israel
[b] Pediatric Neuromuscular Laboratory, Felsenstein Medical Research Center, Tel-Aviv University, 14 Kaplan Street, Petach Tikva 49202, Israel
[c] Department of Pathology, Hadassah-Hebrew-University-Medical-Center, Kiryat Hadassah P.O.B. 12000, Jerusalem 91120, Israel

ARTICLE INFO

Article history:
Accepted 20 July 2019
Available online 16 August 2019

Keywords:
Nerve conduction
Peripheral neuropathy
dy^{2J}/dy^{2J} mice
LAMA2-congenital muscular dystrophy
Glatiramer acetate

HIGHLIGHTS

- dy^{2J}/dy^{2J} mice peripheral neuropathy was confirmed by showing significantly slower NCV than WT.
- Reduced dy^{2J}/dy^{2J} motor NCV improved significantly after GA-treatment.
- The study suggests therapeutic effect for GA in LAMA2-CMD hereditary peripheral neuropathy.

ABSTRACT

Objective: Glatiramer acetate (GA), an agent modulating the immune system, has been shown to cause significantly improved mobility and hind limb muscle strength in the dy^{2J}/dy^{2J} mouse model for LAMA2-congenital muscular dystrophy (LAMA2-CMD). In view of these findings and the prominent peripheral nervous system involvement in this laminin-α2 disorder we evaluated GA's effect on dy^{2J}/dy^{2J} motor nerve conduction electrophysiologically.
Methods: Left sciatic-tibial motor nerve conduction studies were performed on wild type (WT) mice ($n = 10$), control dy^{2J}/dy^{2J} mice ($n = 11$), and GA treated dy^{2J}/dy^{2J} mice ($n = 10$) at 18 weeks of age.
Results: Control dy^{2J}/dy^{2J} mice average velocities (34.49 ± 2.15 m/s) were significantly slower than WT (62.57 ± 2.23 m/s; $p < 0.0005$), confirming the clinical observation of hindlimb paresis in dy^{2J}/dy^{2J} mice attributed to peripheral neuropathy. GA treated dy^{2J}/dy^{2J} mice showed significantly improved average sciatic-tibial motor nerve conduction velocity versus control dy^{2J}/dy^{2J} (50.35 ± 2.9 m/s; $p < 0.0005$).
Conclusion: In this study we show for the first time improvement in motor nerve conduction velocity of LAMA2-CMD dy^{2J}/dy^{2J} mouse model's hereditary peripheral neuropathy following GA treatment.
Significance: This study suggests a possible therapeutic effect of glatiramer acetate on hereditary peripheral neuropathy in this laminin-α2 disorder.

1. Introduction

Laminin-deficient congenital muscular dystrophy (LAMA2-CMD/MDC1A) is inherited autosomal recessively by LAMA2 gene mutations (chromosome 6q22.33), encoding the laminin-α2 subunit of muscle basement membrane protein laminin-211 (merosin) (Collins and Bönnemann, 2010; Helbling-Leclerc et al., 1995), with reduction or complete deficiency of laminin-α2 causing congenital muscular dystrophy demyelinating peripheral neuropathy, and brain white matter changes (Shorer et al., 1995; Tan et al., 1997). Children with this disorder have severe weakness, motor impairment, and joint rigidity (Muntoni and Voit, 2004; Jimenez-Mallebrera, 2005).

Several mouse models for LAMA2-CMD (Table1) display significant muscular dystrophy (Connolly et al., 2001; Gawlik and Durbeej, 2011), and prominent peripheral nervous system (PNS) abnormalities including axonal sorting defect (roots/limb plexuses), severe dysmyelination, lack of basal lamina, and sensory nerves affected less than motor (Bradley et al., 1977; Gawlik and Durbeej, 2011; Harris et al., 1972; Madrid et al., 1975). Electrophysiologic testing reflects this pathology, showing prominent motor nerve conduction velocity (NCV) slowing in the various mouse models (Table 1). In humans with absence or trace amounts of skeletal muscle laminin-α2, there is mild to moderate motor

* Corresponding author at: Institute of Neurology, Schneider Children's Medical Center of Israel, 14 Kaplan Street, Petach Tikva 49202, Israel. Fax: +972 3 9253887.
E-mail address: yoramne@clalit.org.il (Y. Nevo).
[1] Authors contributed equally to the manuscript.

https://doi.org/10.1016/j.clinph.2019.07.029
1388-2457/

Table 1
Normal sciatic-tibial motor NCV data in *dy/dy* and WT mouse models.

Mouse model	Nerve conduction velocity	Reference
dy/dy (unidentified genetic defect)	21 ± 3 m/s – 30 m/s	Huizar et al. (1975), Occhi et al. (2005) and Rasminsky et al. (1978)
dy^{2J}/dy^{2J}	27.7 ± 4.48 m/s – 39 ± 2 m/s	Domi et al. (2015) and Occhi et al. (2005)
dy^{2J}/dy^{2J} *(current study)*	34.49 ± 2.15 m/s	Rabie, Yanay, Fellig, Konikov-Rozenman, Nevo
dy^{3k}/dy^{3k}	19.7 ± 3.1 m/s (27.2 ± 4.4 m/s wild-type control), at 24 °C using different method	Nakagawa et al. (2001)
WT age 12 wk	64.2 ± 5.5 m/s	Dzagnidze et al. (2007)
WT 18 wk (current study)	62.57 ± 2.23 m/s	Rabie, Yanay, Fellig, Konikov-Rozenman, Nevo
WT age 20 wk	55.01 ± 1.88 m/s	Yoon et al. (2009)
WT age 24 wk	52.4 ± 4.6 m/s (ketamine/xylazine anesthesia)	Oh et al. (2010)
WT age 24 wk	62.9 ± 5.7 m/s (isoflurane)	Oh et al. (2010)

NCV slowing, lower-range-of-normal motor NCV, and normal sensory conduction (Matsumura et al., 1997; Shorer et al., 1995). Overall there is approximately 30% NCV slowing in mice and humans with this disorder (Occhi et al., 2005; Rasminsky et al., 1978).

The $Lama^{2dy\text{-}2J}$ (dy^{2J}/dy^{2J}) has a partially functional α2 chain causing a relatively milder phenotype compared to other LAMA2-CMD mouse models, and is useful for studying LAMA2-CMD pathophysiology and therapeutic agent effects (Elbaz et al., 2015; Gawlik and Durbeej, 2011).

Glatiramer acetate (GA) available commercially for immune modulation, can act on the PNS (Aronovich et al., 2012; Zhang et al., 2014) and has been shown to significantly improve mobility and hind limb muscle strength in dy^{2J}/dy^{2J} mice (Dadush et al., 2010). On clinical inspection of these mice it was clear their hindlimb paralysis attributed to peripheral neuropathy was less affected in GA-treated compared to untreated, probably related to attenuation of muscle fibrosis markers and significantly increased expression of muscle regeneration markers (Dadush et al., 2010), or associated with an additional cause such as peripheral nerve. In view of these findings, we evaluated GA's effect on dy^{2J}/dy^{2J} motor peripheral neuropathy myelin and axon parameters by routine nerve conduction without expectation for any specific finding.

2. Materials and methods

2.1. Mice

C57BL/6J $Lama2^{dy\text{-}2J}$ (dy^{2J}/dy^{2J}) heterozygote mice were obtained from Jackson Laboratories (Bar Harbor, ME, USA) and bred at Hebrew University SPF animal housing facility as previously described (Dadush et al., 2010). The Hebrew University Animal Care and Use Committee approved the experiments of this study. Mice were sustained at 23 ± 1 °C, 12-h light cycle (7 a.m.–7 p.m.) with ad libitum access to food and drink and given standard conditions. All the mice were able to reach food and water, and none had paralysis. There was no large weight loss (greater than 10% loss between two weight measurements, or 20% or more from the weight at the beginning of the experiment). No animal had any signs of severe stress that needed to be withdrawn from the study. The treatment group had no problems or side effects. Distinction between dy^{2J}/dy^{2J} mice heterozygous for LAMA2 gene mutation and the wild type C57BL/6J (WT) mice was via PCR reaction with the following primers: forward 5′-TCCTGCTGTCCTGAATCTTG-3′and reverse 5′-CTCTATTACTGAACTTTGGATG-3′. The digestion of the PCR products was broken down with the NdeI restriction enzyme (recognition sequence: CATATG) producing a typical product size for each mouse genotype. dy^{2J}/dy^{2J} mice had 200 μg glatiramer acetate three times a week via intra-peritoneal injection (Copaxone, Teva Pharmaceutical Industries, Petah–Tikva, Israel), and WT and dy^{2J}/dy^{2J} were given saline as control, for a period of 12 weeks, beginning from the age of 6 weeks (WT $n = 10$, control dy^{2J}/dy^{2J} $n = 11$ and GA-treated dy^{2J}/dy^{2J} $n = 10$). Wild type (C57BL/6J) mice previously showed no improvement in mobility/hindlimb strength with GA (Dadush et al., 2010), therefore treatment of WT with GA was not assessed electrophysiologically in the current study. Dosage was determined according to a previous study performed at our laboratory. At the study's end mice were anaesthetized and sacrificed.

Mice were anaesthetized with ketamine-xylazine mix (ketamine 100 mg/kg; xylazine 10 mg/kg). The mix of drugs was injected intraperitoneal (IP) 0.1 ml/10 g bodyweight. If necessary, duration of anesthesia was extended by re-administering ketamine. Anesthetized mice were fixed prone onto silver foil placed on a heating pad, in a temperature controlled room and rectal temperatures were maintained.

2.2. Electrophysiology

Left sciatic-tibial motor nerve conduction studies were performed at 18 weeks of age in the 10 wild type (WT), 11 control dy^{2J}/dy^{2J} and 10 GA-treated dy^{2J}/dy^{2J} mice (200 μg/IP GA given 3/week for 12 weeks, Dadush et al., 2010) using methods adapted from previously described studies (Domi et al., 2015; Dzagnidze et al., 2007; Osuchowski et al., 2009; Yoon et al., 2009). NCS was performed at the 18-week age time point, 12 weeks after GA treatment, based on significant strength and mobility improvement found at this age in treated dy^{2J}/dy^{2J} (Dadush et al., 2010). A Dantec Keypoint®.Net version 2.11, Natus Medical Incorporated, Skovlunde, Denmark, EMG system was used set at sensitivity 2 mv/div., sweep speed 1 ms/div., HFF 5 KHz, and LFF 10 Hz. Anesthetized mice, fixed prone on a heating pad, had left hind limb fixed in extension with natural knee and ankle flexion. Stimulation was by subdermal disposable sensory needle electrodes (SNEs) (Natus® Alpine bioMed, 28G, 15 mm × 0.35 mm) proximally at the sciatic-notch with anode tip introduced 1 mm caudal to the tail-base subcutaneously and advanced about 1 cm, in parallel to the spinal column just lateral to the midline, and cathode about 3 mm lateral and parallel to the anode. Ankle stimulation was performed by SNEs inserted posterior to the medial malleolus (cathode–anode 1 cm apart) with pick-up (G1) SNE in the middle of the fourth interosseous muscle (dorsum of the foot) and reference (G2) SNE subcutaneous in the fourth web space (dorsum). The ground was a disposable monopolar needle electrode (Medtronic®, 26G 37 mm × 0.4 mm) inserted approximately 1 cm subcutaneously at the heel between stimulating cathode (negative pole) and G1. Distal and proximal artefact-free maximal compound muscle action potentials (CMAPs) were obtained with incremental impulse intensity (currents: 15–80 mA, duration: 0.1–0.2 ms). A supramaximal CMAP was obtained by further intensity increment without a concomitant increase in CMAP amplitude. Supramaximal

CMAP amplitudes (peak-to-peak), CMAP area under the negative-peak, CMAP duration (from onset of first negative peak until return to base line of last negative peak), distal and proximal latency (in each case from stimulus artefact to initial onset of the CMAP), and F-wave minimal latencies (from M-wave onset to initial deflection of shortest F-wave) were measured. Nerve conduction velocity (NCV) was calculated by dividing the distance measured with a non-stretchable tape measure along the course of the sciatic-tibial peripheral nerve between distal and proximal cathode stimulation sites, by the difference between sciatic-notch and ankle latencies. Conduction block was defined as >50% drop in proximal CMAP amplitude and area without increased CMAP temporal dispersion. Increased CMAP temporal dispersion was present if proximal CMAP duration was >25% of distal duration.

2.3. Statistical analysis

All data were given as mean ± standard error of the mean (SEM). Statistical analysis was done in SPSS (SPSS 15.0 for windows). Direct comparison between two groups was done by an unpaired Student's *t*-test. Data was analysed also by Kruskal-Wallis test using SAF version 9.4. The results were identical to those found using the student *t*-test. *P*-value for the *F*-wave parameter was also given in Table 2a using Kruskal-Wallis test, because of small sample size. Significance was set at $p < 0.05$ for all comparisons.

3. Results

3.1. Motor nerve conduction studies

3.1.1. General parameters

WT, control dy^{2J}/dy^{2J}, and GA-treated dy^{2J}/dy^{2J} mice showed no significant difference in tail length or rectal temperature (°C). Average core temperatures were maintained at 36.55 ± 0.26 (WT), 36.48 ± 0.27 (dy^{2J}/dy^{2J} control) and 36.85 ± 0.18 (dy^{2J}/dy^{2J} GA). Control and GA-treated dy^{2J}/dy^{2J} weights were similar and significantly lower than WT (Table 2a). Using averages ± SE there was no significant difference for gender in all parameters studied, except for weight (males heavier than females, Table 2b).

3.1.2. Myelin parameters

The 18 week old WT (C57BL/6J) control group average left sciatic-tibial motor NCV (STMNCV) (62.57 ± 2.23 m/s), and average F-wave latency (5.73 ± 0.33 ms) were commensurate with other WT studies (Table 1, Fig. 1F). Control dy^{2J}/dy^{2J} mice average STMNCV was significantly slower (34.49 ± 2.15 m/s; $p < 0.0005$ vs. WT, Fig. 1A), with significantly delayed average F-wave latency (10.88 ± 1.61 ms; $p < 0.05$ vs. WT, Fig. 1F). After GA treatment, dy^{2J}/dy^{2J} mice average motor conduction velocity significantly improved to 50.35 ± 2.9 m/s ($p < 0.0005$ vs control dy^{2J}/dy^{2J}), but remained slower than WT ($p < 0.005$) (Table 2a, Fig. 1A). No conduction block was found in any of the groups. Control dy^{2J}/dy^{2J} mice had significantly increased average proximal CMAP temporal dispersion compared to WT mice (33.55 ± 10.4 % vs. 7.10 ± 2.33 % $p = 0.009$, respectively) (Table 2a, Fig. 1B). GA treated dy^{2J}/dy^{2J} had average proximal CMAP temporal dispersion (32.95 ± 15.6%) similar to the untreated control dy^{2J}/dy^{2J} group but with high variation inside the group, thus there was no significant difference between treated dy^{2J}/dy^{2J} vs. dy^{2J}/dy^{2J} and WT control groups (Fig. 1B). Average ankle distal latency difference between WT and dy^{2J}/dy^{2J} control groups did not reach statistical significance (WT 1.01 ± 0.04 ms; control dy^{2J}/dy^{2J} 1.37 ± 0.31 ms, Fig. 1E). GA-treated dy^{2J}/dy^{2J} mice average distal latencies showed a tendency towards improvement compared to control dy^{2J}/dy^{2J} (Table 2a and Fig. 1E). Fig. 2 shows nerve conduction tracings with prominent NCV slowing in dy^{2J}/dy^{2J} compared to WT, with NCV improvement after GA-treatment.

3.1.3. Axonal parameters

Sciatic-tibial nerve CMAP amplitudes of control and GA-treated dy^{2J}/dy^{2J} (1.78 ± 0.4 mv, 1.31 ± 0.32 mv, respectively) and CMAP areas were significantly lower than WT mice (amplitude: 6.01 ± 1.357 mv; $p < 0.05$, Table 2a, and Fig. 1G and H), with no improvement after GA treatment.

4. Discussion

We have validated and characterized electrophysiologically the neuropathy of the dy^{2J}/dy^{2J} mouse model by showing that 18 week old dy^{2J}/dy^{2J} mice had significantly reduced average motor nerve conduction velocity, increased proximal CMAP temporal

Table 2a
Nerve conduction data.

	Type Wild ($n = 10$)	dy^{2J}/dy^{2J} CTRL ($n = 11$)	dy^{2J}/dy^{2J} GA ($n = 10$)
General Parameters			
Weight (gr)	26.66 ± 0.99	20.25 ± 0.86**	19.77 ± 0.59**
Tail length (cm)	7.59 ± 0.09	7.65 ± 0.10	7.72 ± 0.15
Temp. C (rectal)	36.55 ± 0.26	36.48 ± 0.27	36.85 ± 0.18
Male ; Female	7 ; 3	4 ; 7	5 ; 5
Myelin Parameters			
Nerve Conduction Velocity (NCV) (m/s)	62.57 ± 2.23	34.49 ± 2.15***	50.35 ± 2.9**/#
NCV range (m/s)	46–73.8	20.6–48	36.3–66.7
% Increased Proximal CMAP Temporal Dispersion (abnormal >25%)	7.10 ± 2.33	33.55 ± 10.4*	32.95 ± 15.6
Distal CMAP Duration (ms)	2.65 ± 0.22	3.01 ± 0.56	2.81 ± 0.23
Proximal CMAP Duration (ms)	2.78 ± 0.2	3.73 ± 0.55	3.66 ± 0.57
Ankle Distal Latency (ms)	1.01 ± 0.04	1.37 ± 0.31	1.084 ± 0.07
F-wave Minimal Latency from ankle (ms)	5.73 ± 0.33 ($n = 10$)	10.88 ± 1.61* ($n = 5$)	9.65 ± 1.92 ($n = 4$)
Axonal parameters			
Distal CMAP Amplitude (mv)	6.01 ± 1.357	1.78 ± 0.40*	1.31 ± 0.32*
Distal CMAP Area (mv.ms)	1.77 ± 0.36	0.61 ± 0.12*	0.54 ± 0.11*

The mean value and the standard error of mean (SEM) is presented. Student's *t*-test; *$p < 0.05$, **$p < 0.005$, ***$p < 0.0005$ vs. wild type group, #$p < 0.0005$ vs. dy^{2J}/dy^{2J} CTRL group. All other comparisons were not significant. Using Kruskal-Wallis test for F-wave, dy^{2J}/dy^{2J} CTRL vs. wild type group *p*-value < 0.01. CMAP = compound muscle action potential.

Table 2b
Nerve conduction data according to mice gender.

	WT ($n = 10$)			dy^{2J}/dy^{2J} CTRL ($n = 11$)			dy^{2J}/dy^{2J} GA ($n = 10$)		
	Male	*Female*	*p-value*	*Male*	*Female*	*p-value*	*Male*	*Female*	*p-value*
Weight (g)	28.47 ±0.003 ($n = 7$)	22.43 ±0.745 ($n = 3$)	0.005*	23.45 ±0.5 ($n = 4$)	18.39 ±0.55 ($n = 7$)	0.0001*	20.896 ± 0.57 ($n = 5$)	18.64 ±0.8 ($n = 5$)	0.05*
NCV (m/s)	61.77 ±3.4 ($n = 7$)	64.43 ±0.23 ($n = 3$)	*N.S* 0.46	31.175 ± 3.96 ($n = 4$)	35.81 ±2.5 ($n = 7$)	*N.S* 0.36	52.47 ±3.7 ($n = 5$)	48.22 ±4.7 ($n = 5$)	*N.S* 0.49
Proximal CMAP % Dispersion	9 ± 2.9 ($n = 7$)	2.66 ± 2.67 ($n = 3$)	*N.S* 0.16	44.25 ±25 ($n = 4$)	27.428 ± 9.3 ($n = 7$)	*N.S* 0.56	13.625 ± 6.05 ($n = 5$)	52 ±29.7 ($n = 5$)	*N.S* 0.24
F-wave (ms)	5.38 ±0.28 ($n = 7$)	6.53 ±0.81 ($n = 3$)	*N.S* 0.29	7.4 ±1.2 ($n = 2$)	13.2 ±1.12 ($n = 3$)	*N.S* 0.051	6.9 ±0.4 ($n = 2$)	10.7 ±2.27 ($n = 2$)	*N.S* 0.23
CMAP Amplitude (mv)	4.43 ± 0.51 ($n = 7$)	9.7 ± 4.01 ($n = 3$)	*N.S* 0.32	1.3 ±0.58 ($n = 4$)	2.057 ±0.57 ($n = 7$)	*N.S* 0.38	1.2 ±0.49 ($n = 5$)	1.42 ±0.52 ($n = 5$)	*N.S* 0.77
CMAP Area (ms.mv)	1.279 ±0.19 ($n = 7$)	2.93 ±0.98 ($n = 3$)	*N.S* 0.23	0.45 ±0.17 ($n = 4$)	0.728 ±0.16 ($n = 7$)	*N.S* 0.28	0.5 ±0.17 ($n = 5$)	0.58 ±0.19 ($n = 5$)	*N.S* 0.76

There were no gender differences in all parameters tested except for body weight. Data is given as mean value and the standard error of mean (SEM).

dispersion, and increased F wave latency compared to WT mice (Table 1 and Table 2a). There was no conduction block, indicating that there is similar pathology in different segments of the nerve, as can be expected in a hereditary peripheral neuropathy. Our average control dy^{2J}/dy^{2J} NCV showed slowing of approximately 45% compared to WT which is commensurate with the approximate 30% NCV slowing reported previously in studies of dy^{2J}/dy^{2J} mice of varying ages, small numbers, and very little normative data available (Table 1 and Fig. 1A). In addition, previous studies used different temperatures/anaesthetic agents, and in some cases different nerves (tail nerve) compared to the current study. Huizar et al., (1975), showed *dy/dy* NCV of spinal motor neurones remained unchanged between ages 63–148 days (9–21 weeks), while control mice aged 69–90 days (9.85–12.85 weeks) mean NCV was significantly slower (43 m/s) than mice older than 100 days (14.28 weeks; 53 m/s). This increase in NCV with age in normal mice without an increase in NCV in *dy/dy* mice with age, may play a role in the increased difference of 44.87% found between our 18 week old dy^{2J}/dy^{2J} versus WT, compared to approximate 30% difference found in other studies done at an earlier age. No conclusions regarding the progression of the neuropathy can be drawn from our data or from previous data, as our dy^{2J}/dy^{2J} average NCV and F-wave latency at 18 weeks of age (Table 2a and Fig. 1A and F) are similar to previous studies done between ages approximately 45 days to 12 weeks, with NCVs ranging from 27.71 ± 4.84 to 39 ± 2 m/s (Table 1). The WT normative sciatic-tibial motor NCV data (average 62.57 ± 2.23 m/s) in our study was similar to previous WT data (Fig. 1A, Table 2a, Table 1) (Sullivan et al., 2008).

Following a previous study in which we showed significant mobility and strength improvement after GA treatment in dy^{2J}/dy^{2J} mice (Dadush et al., 2010), we found in this project significantly improved NCV following GA treatment (treated dy^{2J}/dy^{2J} mice versus control dy^{2J}/dy^{2J} $p < 0.0005$ as shown in Table 2a and Fig. 1A).

The approximate 35.6% prolongation of the average distal latency in control dy^{2J}/dy^{2J} compared to WT (not statistically significant) suggests diffuse NCV slowing along the course of the sciatic-tibial nerve, as expected in a hereditary neuropathy. The control dy^{2J}/dy^{2J} distal latency tended to improve after GA-treatment (not statistically significant). Average F-wave latencies did not show improvement in GA-treated versus control dy^{2J}/dy^{2J}. Severe ventral spinal root NCV slowing (NCV approximately 2.3 m/s) occurring in the *dy/dy* mouse model (Huizar et al., 1975; Jaros and Jenkison, 1983; Matsumura et al., 1997; Yang et al., 2005), may be a reason why the significant increase in STMNCV in GA-treated dy^{2J}/dy^{2J} is not reflected in a faster F-wave conduction time.

The CMAP amplitude and area, indicators of the number of depolarized myelinated motor axons and their activated muscle fibers, were significantly reduced ($p < 0.05$) in control and GA-treated dy^{2J}/dy^{2J} mice compared to WT, without significant difference between the control and treated dy^{2J}/dy^{2J} groups (Table 2a and Fig. 1G and H).

The molecular and pathological basis for the reduced NCV in dy^{2J}/dy^{2J} mice and patients with laminin-α2 mutations may involve specific Schwann cell laminins, receptors and cytoskeletal linkage that participate in the formation of a transcellular scaffold important for assembly of nodal architecture (Gawlik and Durbeej, 2011; Occhi et al., 2005). Reduced myelinated axon density (Montgomery and Swenarchuk, 1978), reduction in internodal length (Di Muzio et al., 2003; Jaros and Jenkison, 1983), widened nodes of Ranvier (Bradley et al., 1977; Jaros and Jenkison, 1983), probable reduction in node of Ranvier Nav channel density in the distal PNS (Occhi et al., 2005), amyelination more pronounced in spinal roots (but also present in sciatic nerve) due to defective radial sorting (Matsumura et al., 1997; Stirling, 1975; Yang et al., 2005), severe dysmyelination, lack of PNS basal lamina, and in some mouse models smaller axon diameter may contribute to the pathogenesis of the NCV slowing in this laminin-α2 disorder (Di Muzio et al., 2003; Madrid et al., 1975; Nakagawa et al., 2001; Occhi et al., 2005). Interestingly, the complexity of the causation of peripheral neuropathy in LAMA2-CMD is reflected by the dy^{nmf417}/dy^{nmf417} model ($Lama2^{dy\text{-}7J}$) which has normal-α2 chain levels, mild muscular dystrophy, but prominent PNS pathology (Patton et al., 2008). This model has no disruption of basal laminal ultrastructural integrity on myelinating Schwann cells or muscle fibers, suggesting dysmyelination/amyelination from laminin-α2 mutations may not simply be related to basal lamina compromise or reduction in laminin-α2 (Patton et al., 2008; Yang et al., 2005). The mechanism of the clinical and electrophysiological improvement following GA treatment shown in this dy^{2J}/dy^{2J} mouse model of LAMA2-CMD, is currently unknown.

Even though the exact mechanism of GA in general has never been substantiated, GA has proven efficacy in improving the course of the disease in relapsing remitting multiple sclerosis (MS) patients (Lalive et al., 2011). GA simulates myelin basic protein and improves outcome in both EAE mouse and rat EAN models (Aronovich et al., 2012; Robinson et al., 2014). For GA, an immune modulating pathogenesis is commonly postulated involving differ-

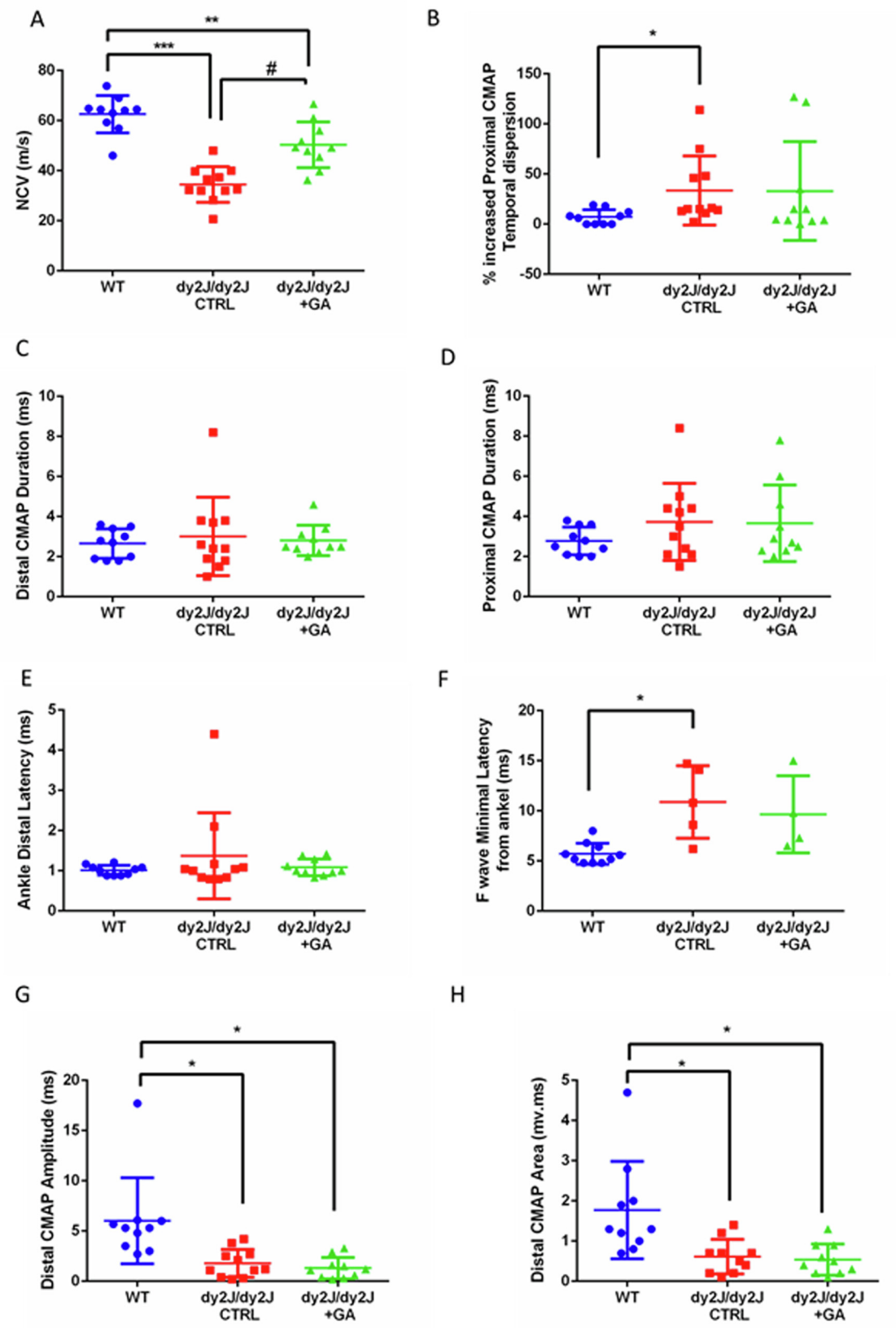

Fig. 1. Nerve conduction parameters. A to F representing myelin parameters and G to H axonal parameters. (A) Nerve conduction velocity (NCV) measurements. GA treated dy^{2J}/dy^{2J} mice average NCV significantly improved compared to the untreated group but remained slower than WT mice. (B) % Increased Proximal CMAP Temporal Dispersion (abnormal > 25%). (C) Distal CMAP Duration (ms). (D) Proximal CMAP Duration (ms). (E) Ankle Distal Latency (ms). (F) F-wave Minimal Latency from ankle (ms). (G) Distal CMAP Amplitude (mv). (H) Distal CMAP Area (mv.ms). Student's *t*-test; $^{**}p < 0.005$, $^{***}p < 0.0005$, $\#p < 0.0005$.

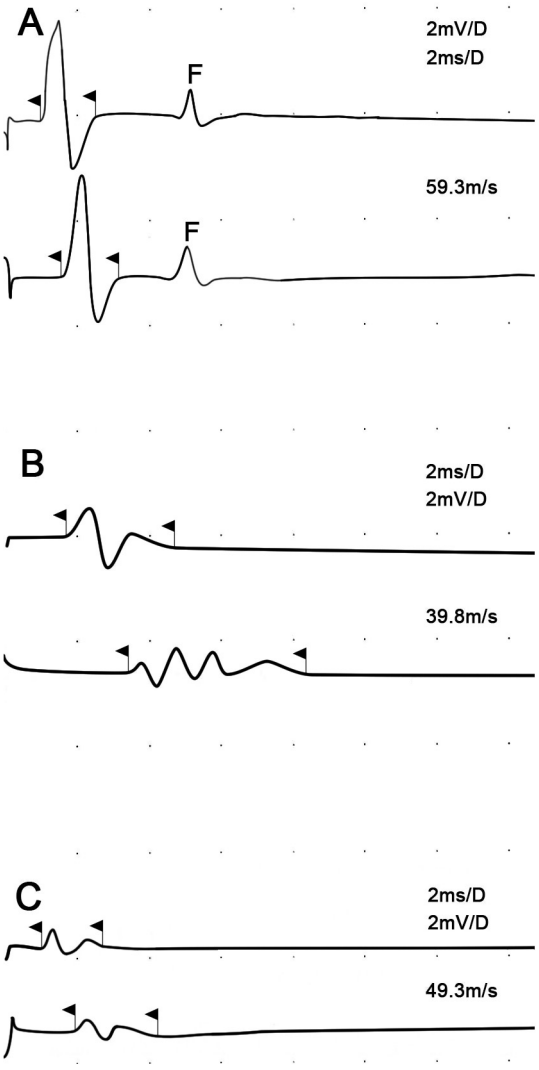

Fig. 2. Sciatic-tibial motor nerve conduction demonstrating low CMAP amplitudes and NCV slowing in dy^{2J}/dy^{2J}. (A) WT, (B) Untreated dy^{2J}/dy^{2J}, (C) GA-treated dy^{2J}/dy^{2J} NCV improvement. Flags = markers of CMAP onset and return to baseline, F = F-wave.

ent pathways both inside of the nervous system and outside (Arnon et al., 2004; Aronovich et al., 2012; Dadush et al., 2010).

However, GA has been shown to produce positive effect in non-immune mediated disorders, and may have direct neuroprotective and/or remyelinating properties, presumably through an upregulation of neurotrophic factors (Arnon et al., 2004; Dadush et al., 2010; Lalive et al., 2011). Glatiramer acetate normalizes microRNA expression (miR-146a and miR-142-3p, regulators of immune tolerance) in relapsing remitting MS (Waschbisch et al., 2011). MicroRNAs, short non-coding RNAs that modulate gene expression post-transcriptionally, are also implicated in the regulation of peripheral nerve myelination, with roles in transition from immature to myelinating Schwann cell, as well as regulation of peripheral myelin protein 22 (Gokey et al., 2011; Verrier et al., 2009). Since GA can affect microRNA expression in the CNS (Waschbisch et al., 2011), and microRNAs are involved in peripheral nerve myelination (Gokey et al., 2011; Verrier et al., 2009), this together with the fact that GA has been shown to act on the PNS (Aronovich et al., 2012; Zhang et al., 2014), it may be possible that GA could have a mechanism of action also via microRNAs on the PNS in this mouse model for LAMA2-CMD. Possible GA mechanisms in this mouse model may include a compensatory upregulation of other laminin chains upon treatment, inactivation of proapoptosis pathways, or changes to protein kinase A activation. Limitations of this study include small sample size, missing longitudinal comparison and follow-up data, as well as a lack of histology and molecular analysis. In summary, GA's mechanism of action is not known in the dy^{2J}/dy^{2J} mouse, and may occur via inhibition of inflammatory processes and/or anti-fibrosis effects in the muscle, and neuroprotective effect or enhanced regeneration in the peripheral neuropathy in this model (Dadush et al., 2010).

5. Conclusion

Following clinical observation of hindlimb paresis attributed to neuropathy in dy^{2J}/dy^{2J} mice, we have re-confirmed electrophysiologically the presence of neuropathy in this model. In this study we show for the first time improvement in peripheral motor nerve conduction velocity following GA treatment. Improved dy^{2J}/dy^{2J} NCV does not explain the improved muscle strength previously described by Dadush et al. (2010), but it may have some baring on the improved mobility that was observed, via faster reflex pathways. Showing improved velocity demonstrates the usefulness of nerve conduction studies in quantitating potential pharmacological effects on peripheral nerve demyelination in neuropathies. The mechanism of GA's effect is yet to be elucidated.

Study funding

This work was supported in part by the NNE grant program of Teva Pharmaceutical. Teva Pharmaceutical had no involvement in the study design, in the collection, in the analysis and in the interpretation of data, in the writing of the report, or in the decision to submit the article for publication.

Author contributions

MR – Initiated the project, performed nerve conduction studies, wrote the manuscript.
NY – Performed all mice experiments, wrote the manuscript.
JKR – Performed mice experiments, revised the manuscript.
YF – Revised the manuscript.
YN - Initiated the project, wrote the manuscript.

Declaration of Competing Interest

The authors declare that they have no conflict of interest.
Prof. Nevo has an international PCT patent (application no. PCT/IL2008/001289) on GA treatment in muscular dystrophy; however, it does not include the effects of GA on central and peripheral nervous system.

References

Aronovich R, Katzav A, Chapman J. The strategies used for treatment of experimental autoimmune neuritis (EAN): a beneficial effect of glatiramer acetate administered intraperitoneally. Clin Rev Allergy Immunol 2012;42:181–8.
Arnon R, Aharoni R. Mechanism of action of Glatiramer acetate in multiple sclerosis and its potential for the development of new applications. PNAS 2004;101:14593–8.
Bradley WG, Jaros E, Jenkison M. The nodes of Ranvier in the nerves of mice with muscular dystrophy. J Neuropathol Exp Neurol 1977;36:797–806.
Collins J, Bönnemann CG. Congenital muscular dystrophies: toward molecular therapeutic interventions. Curr Neurol Neurosci Rep 2010;10:83–91.
Connolly AM, Keeling RM, Mehta S, Pestronk A, Sanes JR. Three mouse models of muscular dystrophy: the natural history of strength and Fatigue in dystrophin-, dystrophin/utrophin-, and laminin alpha2-deficient mice. Neuromuscul Disord 2001;11:703–12.
Dadush O, Aga-Mizrachi S, Ettinger K, Tabakman R, Elbaz M, Fellig Y, et al. Improved muscle strength and mobility in the dy(2J)/dy(2J) mouse with merosin deficient

congenital muscular dystrophy treated with Glatiramer acetate. Neuromuscul Disord 2010;20:267–72.
Di Muzio A, De Angelis MV, Di Fulvio P, Ratti A, Pizzuti A, Stuppia L, et al. Dysmyelinating sensory-motor neuropathy in merosin-deficient congenital muscular dystrophy. Muscle Nerve 2003;27:500–6.
Domi T, Porrello E, Velardo D, Capotondo A, Biffi A, Tonlorenzi R, et al. Mesoangioblast delivery of miniagrin ameliorates murine model of merosin deficient congenital muscular dystrophy type 1A. Skeletal Muscle 2015;5:30. https://doi.org/10.1186/s13395-015-0055-5.
Dzagnidze A, Katsarava Z, Makhalova J, Liedert B, Yoon MS, Kaube H, et al. Repair capacity for platinum-DNA adducts determines the severity of cisplatin-induced peripheral neuropathy. J Neurosci 2007;27:9451–7.
Elbaz M, Yanay N, Laban S, Rabie M, Mitrani-Rosenbaum S, Nevo Y. Life or death by NFκB, Losartan promotes survival in dy2J/dy2J mouse of MDC1A. Cell Death Dis 2015;6:e1690.
Gawlik KI, Durbeej M. Skeletal muscle laminin and MDC1A: pathogenesis and treatment strategies. Skelet Muscle 2011;1:1–9.
Gokey NG, Srinivasan R, Lopez-Anido C, Krueger C, Svaren J. Developmental regulation of microRNA expression in Schwann Cells. Mol Cell Biol 2011;32:558–68.
Harris JB, Wallace C, Wing J. Myelinated nerve fibre counts in the nerves of normal and dystrophic mouse muscle. J Neurol Sci 1972;15:245–9.
Helbling-Leclerc A, Zhang X, Topaloglu H, Cruaud C, Tesson F, Weissenbach J, et al. Mutations in the laminin alpha 2-chain gene (LAMA2) cause merosin- deficient congenital muscular dystrophy. Nat Genet 1995;11:216–8.
Huizar P, Kuno M, Miyata Y. Electrophysiological properties of spinal motoneurones of normal and dystrophic mice. J Physiol 1975;248:231–46.
Jaros E, Jenkison M. Quantitative studies of the abnormal axon-Schwann cell relationship in the peripheral motor and sensory nerves of the dystrophic mouse. Brain Res 1983;258:181–96.
Jimenez-Mallebrera C, Brown SC, Sewry CA, Muntoni F. Congenital muscular dystrophy: molecular and cellular aspects. Cell Mol Life Sci 2005;62:809–23.
Lalive PH, Neuhaus O, Benkhoucha M, Burger D, Hohlfeld R, Zamvil SS, et al. Glatiramer acetate in the treatment of multiple sclerosis: emerging concepts regarding its mechanism of action. CNS Drugs 2011;25:401–14.
Madrid RE, Jaros E, Cullen MJ, Bradley WG. Genetically determined defect of Schwann cell basement membrane in dystrophic mice. Nature 1975;257:319–21.
Matsumura K, Yamada H, Saito F, Sunada Y, Shimizu T. Peripheral nerve involvement in merosin-deficient congenital muscular dystrophy and dy mouse. Neuromuscul Disord 1997;7:7–12.
Montgomery A, Swenarchuk L. Further observations on myelinated axon numbers in normal and dystrophic mice. J Neurol Sci 1978;38:77–82.
Muntoni F, Voit T. The congenital muscular dystrophies in 2004: a century of exciting progress. Neuromuscul Disord 2004;14:635–49.
Nakagawa M, Miyagoe-Suzuki Y, Ikezoe K, Miyata Y, Nonaka I, Harii K, et al. Schwann cell myelination occurred without basal lamina formation in laminin alpha2 chain-null mutant (dy3K/dy3K) mice. Glia 2001;35:101–10.
Occhi S, Zambroni D, Del Carro U, Amadio S, Sirkowski EE, Scherer SS, et al. Both laminin and Schwann cell dystroglycan are necessary for proper clustering of sodium channels at nodes of Ranvier. J Neurosci 2005;25:9418–27.
Oh SS, Hayes JM, Sims-Robinson C, Sullivan KA, Feldman EL. The effects of anesthesia on measures of nerve conduction velocity in male C57Bl6/J mice. Neurosci Lett 2010;483:127–31.
Osuchowski MF, Teener J, Remick D. Noninvasive model of sciatic nerve conduction in healthy and septic mice: reliability and normative data. Muscle Nerve 2009;40:610–6.
Patton BL, Wang B, Tarumi YS, Seburn KL, Burgess RW. A single point mutation in the LN domain of LAMA2 causes muscular dystrophy and peripheral amyelination. J Cell Sci 2008;121:1593–604.
Rasminsky M, Kearney RE, Aguayo AJ, Bray GM. Conduction of nervous impulses in spinal roots and peripheral nerves of dystrophic mice. Brain Res 1978;143:71–85.
Robinson AP, Harp CT, Noronha A, Miller SD. The experimental autoimmune encephalomyelitis (EAE) model of MS: utility for understanding disease pathophysiology and treatment. Handb Clin Neurol 2014;122:173–89.
Shorer Z, Philpot J, Muntoni F, Sewry C, Dubowitz V. Demyelinating peripheral neuropathy in merosin-deficient congenital muscular dystrophy. J Child Neurol 1995;10:472–5.
Stirling CA. Experimentally induced myelination of amyelinated axons in dystrophic mice. Brain Res 1975;87:130–5.
Sullivan KA, Lentz Jr SI, Roberts JL, Feldman EL. Criteria for creating and assessing mouse models of diabetic neuropathy. Curr Drug Targets 2008;9:3–13.
Tan E, Topaloglu H, Sewry C, Zorlu Y, Naom I, Erdem S, et al. Late onset muscular dystrophy with cerebral white matter changes due to partial merosin deficiency. Neuromuscul Disord 1997;7:85–9.
Verrier JD, Lau P, Hudson L, Murashov AK, Renne R, Notterpek L. Peripheral Myelin protein 22 is regulated post-transcriptionally by miRNA-29a. Glia 2009;57:1265–79.
Waschbisch A, Atiya M, Linker RA, Potapov S, Schwab S, Derfuss T. Glatiramer acetate treatment normalizes deregulated microRNA expression in relapsing remitting multiple sclerosis. PLoS One 2011;6:e24604.
Yang D, Bierman J, Tarumi YS, Zhong YP, Rangwala R, Proctor TM, et al. Coordinate control of axon defasciculation and myelination by laminin-2 and -8. J Cell Biol 2005;168:655–66.
Yoon MS, Katsarava Z, Obermann M, Schäfers M, Liedert B, Dzagnidze A, et al. Erythropoietin overrides the triggering effect of DNA platination products in a mouse model of cisplatin-induced neuropathy. BMC Neurosci 2009;10:77. https://doi.org/10.1186/1471-2202-10-77.
Zhang CJ, Zhai H, Yan Y, Hao J, Li MS, Jin WN, et al. Glatiramer acetate ameliorates experimental autoimmune neuritis. Immunol Cell Biol 2014;92:164–9.